**Smart Structures and Systems**, *Vol. 21, No. 6 (2018) 741-749*
DOI: https://doi.org/10.12989/sss.2018.21.6.741


# Sparsity-constrained Extended Kalman Filter concept for damage localization and identification in mechanical structures

Daniel Ginsberg[*1], Claus-Peter Fritzen[2a] and Otmar Loffeld[3b]

*[1]Department of Mechanical Engineering, University of Siegen, Paul-Bonatz-Strasse 9-11, 57076 Siegen, Germany*
*[2]Department of Mechanical Engineering and Center of Sensor Systems (ZESS), University of Siegen, Paul-Bonatz-Strasse 9-11, 57076 Siegen, Germany*
*[3]Center of Sensor Systems (ZESS), University of Siegen, Paul-Bonatz-Strasse 9-11, 57076 Siegen, Germany*

*(Received November 30, 2017, Revised April 27, 2018, Accepted April 30, 2018)*

**Abstract.** Structural health monitoring (SHM) systems are necessary to achieve smart predictive maintenance and repair planning as well as they lead to a safe operation of mechanical structures. In the context of vibration-based SHM the measured structural responses are employed to draw conclusions about the structural integrity. This usually leads to a mathematically ill-posed inverse problem which needs regularization. The restriction of the solution set of this inverse problem by using prior information about the damage properties is advisable to obtain meaningful solutions. Compared to the undamaged state typically only a few local stiffness changes occur while the other areas remain unchanged. This change can be described by a sparse damage parameter vector. Such a sparse vector can be identified by employing $L_1$-regularization techniques. This paper presents a novel framework for damage parameter identification by combining sparse solution techniques with an Extended Kalman Filter. In order to ensure sparsity of the damage parameter vector the measurement equation is expanded by an additional nonlinear $L_1$-minimizing observation. This fictive measurement equation accomplishes stability of the Extended Kalman Filter and leads to a sparse estimation. For verification, a proof-of-concept example on a quadratic aluminum plate is presented.

**Keywords:** $L_1$-minimization; sparse reconstruction; Extended Kalman Filter; damage identification

## 1. Introduction

Structural health monitoring (SHM) is a methodology to ensure a safe operation of mechanical structures and to reduce life cycle cost by replacing schedule-driven inspections by Condition-Based Maintenance (CBM). One major task of SHM systems is the detection and identification of damage in an early stage of structural damage evolution. For vibration-based SHM an integrated sensor network is required to measure the structural vibrations excited either by an artificial or a natural source, e.g. wind and traffic loads. By means of the integrated sensor system the effect of the damage on the structural vibration response can be measured. Now, SHM systems need smart data processing algorithms in order to draw conclusions about the exact cause for the measured effect. Thus, vibration-based damage identification can be seen as the inversion of the principle of cause and effect. This leads to a mathematical inverse problem.

If there are many causes which will lead to the same measurable effect, the inverse problem is additionally ill-posed. Ill-posedness means that either the existence, the uniqueness or the stability of the solution is violated.

In the last decades many methods have been developed and a considerable amount of literature has been published on the inverse problem of structural damage identification, an overview on this topic can be found for example in (Sohn *et al*. 2003) and (Balageas *et al.* 2006). Damage identification techniques can be classified as frequency or time domain or time-frequency domain methods. Classical frequency domain approaches consider the changes of the natural frequencies, modal damping and mode shapes due to damage. As these quantities provide information on a global level, they are often insensitive to small local structural damage. Especially if only lower structural modes are used. In the medium or higher frequency range problems may occur to identify these modes since this requires a very dense sensor network. Time domain approaches seem to be comfortable, as raw time data can be used directly.

Several time domain approaches have already been proposed, such as least-squares estimation methods (Smyth *et al*. 1999, Yang and Lin 2005) or methods using particular filters (Wu and Wang 2014, Wan *et al*. 2013, Ching *et al.* 2006, Sato and Qi 1998). For the latter the Extended Kalman filter (EKF) is the most well-known system parameter estimation method (Ding and Guo 2016, Lei *et al*. 2015, Corigliano and Mariani 2004, Liu *et al.* 2009, Lei *et al*. 2013). EKF-based system parameter identification belongs to the class of model-based approaches. Here, a reference model of the undamaged structure is tested

∗Corresponding author, Ph.D. Student
E-mail: daniel.ginsberg@uni-siegen.de
[a] Professor
E-mail: claus-peter.fritzen@uni-siegen.de
[b] Professor
E-mail: loffeld@zess.uni-siegen.de


http://www.techno-press.com/journals/sss&subpage=7
ISSN: 1738-1584 (Print), 1738-1991 (Online)

against the actual system in each filter step. In the filter process the state vector of the Kalman Filter equations is typically augmented (Liu *et al.* 2009) or sometimes even replaced (Ebrahimian *et al.* 2015) by the system parameter to be estimated. By making use of the input-output signal an estimation of the system parameters is obtained in each filter step. Even so the original Kalman Filter is known as optimal linear filter, EKF-based damage identification is still facing some challenges, e.g. high computational effort for complex structures and intrinsic ill-posedness of the inverse problem (Zhang *et al.* 2016). To overcome ill-posedness usually the damage parameter space is reduced by considering only damage hot spots or by a drastic increase of the sensor number. In order to perform damage monitoring on the whole structure and to keep the required number of sensors low, a sparsity-constrained Extended Kalman Filter concept is proposed.

Therefore, a priori information about the damage properties is used to solve the inverse problem and to obtain meaningful solutions. For example, cracks can be interpreted as spatial singularities, which cause only a very local structural stiffness reduction. Thus, a system parameter vector which describes the change in structural stiffness has only a few non-zeros elements corresponding to the actual damage location. Such a vector is called sparse. In many fields of applied mathematics, $L_1$-regularizing techniques have been proven to promote such kind of sparse solutions (e.g., Compressive Sensing (Candès and Wakin 2008, Donoho and Huo 2006)). The proposed damage identification method links the concept of $L_1$-regularization with the Extended Kalman Filter by expanding the measurement equation by an additional nonlinear $L_1$-minimizing observation.

The paper is structured as follows: Section 2 describes the $L_1$-minimizing sparse solution strategy for inverse problems. The problem of damage parameter estimation using a non-linear state-space description is formulated in section 3. In section 4 the concept of sparse solution is incorporated in the Extended Kalman Filter concept. Various proof-of-concept simulation studies are carried out in section 5. Here the functionality of the proposed identification method is demonstrated by analyzing different damaged scenarios on a quadratic aluminum plate structure. A stochastic validation is performed by means of a Monte Carlo simulation and the capability of compensating modeling errors is also shown. Finally, concluding remarks are presented in section 6.

## 2. Sparse solution of inverse problem

Most ill-posed inverse problems can be formulated by a linear algebraic equation system of the form

$$\boldsymbol{y} = \boldsymbol{H} \cdot \boldsymbol{A} \tag{1}$$

or can be transformed into such a system. In Eq. (1) $\boldsymbol{y} \in \mathbb{R}^M$ is a vector which contains all measurable output information and $\boldsymbol{A} \in \mathbb{R}^N$ is a vector containing all possible causes or inputs, respectively. The transition matrix $\boldsymbol{H} \in \mathbb{R}^{M \times N}$ describes the linear effect-causes relationship. If the dimension of $\boldsymbol{y}$ is smaller than the dimension of $\boldsymbol{A}\,(M < N)$ the linear system of equation is underdetermined. In this case Eq. (1) has an infinite number of possible solutions, which means an infinite number of different causes will result in the same effect. The challenge of solving such an equation system is the determination of the actual one.

In order to close the gap of information and to obtain a solution, additional constraints $\Omega(\boldsymbol{A})$ need to be formulated, which regularize the problem. The most common regularization is the Tikhonov regularization (Tikhonov and Arsenin 1977)

$$\hat{\boldsymbol{A}}_2 = \underset{\boldsymbol{A} \in \mathbb{R}^N}{\arg\min} \left\{ \|\boldsymbol{y} - \boldsymbol{H} \cdot \boldsymbol{A}\|_2^2 + \lambda \|\boldsymbol{A}\|_2^2 \right\} \tag{2}$$

with the constraint $\Omega(\boldsymbol{A})$

$$\Omega(\boldsymbol{A}) = \|\boldsymbol{A}\|_2^2 \quad \text{and} \quad \|\boldsymbol{A}\|_2^2 = \sqrt{\sum_i A_i^2} \tag{3}$$

Here, the solution of Eq. (1) is generated via an optimization problem. The constraint can be interpreted as additional information which regularize the inverse problem and forces the $L_2$-norm (or Euclidian norm) of the solution vector $\hat{\boldsymbol{A}}_2$ to be minimal. Furthermore, for Tikhonov regularization $\boldsymbol{y}$ is not necessarily equal $\boldsymbol{H} \cdot \boldsymbol{A}$ so that the solution is stabilized if $\boldsymbol{y}$ is polluted by noise. However, for most applications the choice of $L_2$-minimization as constraint is not suitable to close the gap of information and to obtain meaningful results.

In recent years, new reconstruction strategies for solving underdetermined linear systems of equations have been proposed, pushed forward by the developments in the field of Compressive Sensing (CS) (Candès and Wakin 2008, Donoho and Huo 2006). For these reconstruction methods it is assumed that the solution vector has just a few nonzero elements or can be transformed to such a sparse vector by using some other coordinate spaces. This assumption holds for most vectors which describe some real-world phenomena (e.g., images, sounds, forces); the elements inside such vectors are not completely arbitrary and have some kind of internal structure. Such a structure is always used for compressing data, e.g., wavelet transformation of images or Fourier transformation of sounds. So the information carried by these vectors is mostly a lot smaller than the dimension of the vectors itself suggests. However, it is not known in advance which elements are nonzero, but the information that the solution vector is sparse can be included as additional information in the reconstruction strategy (Fritzen and Ginsberg 2017).

The numbers of nonzero elements inside the vector $\boldsymbol{A}$ can be expressed by means of the $L_0$-norm

$$s = \|\boldsymbol{A}\|_0 = |\mathrm{supp}(\boldsymbol{A})| \tag{4}$$

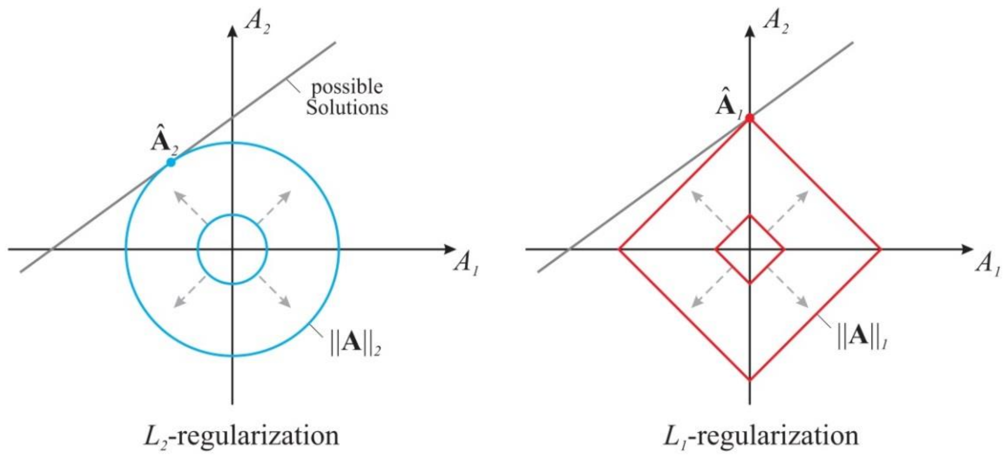


Fig. 1 Comparison of $L_2$- and $L_1$-regularization of underdetermined equation systems

where $|\text{supp}(\boldsymbol{A})| := \{i : A_i \neq 0\}$ denotes the support set of the vector $\boldsymbol{A}$ and $|\circ|$ the cardinality of this set. If the dimension $N$ of the vector $\boldsymbol{A}$ is much bigger than the number of nonzero elements $s\,(N >> s)$, then $\boldsymbol{A}$ is a sparse vector.

The sparsest solution which agrees with the measurements $\boldsymbol{y}$ could be obtained by minimizing the following expression

$$\hat{\boldsymbol{A}}_{\boldsymbol{0}} = \underset{\boldsymbol{A} \in \mathbb{R}^N}{\arg\min} \|\boldsymbol{A}\|_0 \qquad \text{subject to} \qquad \boldsymbol{y} = \boldsymbol{H} \cdot \boldsymbol{A} \tag{5}$$

Unfortunately, solving Eq. (5) requires a combinatorial search, which makes it nearly impossible to solve computationally for larger values of $N$. Under the assumption of a sparse solution, e.g., in (Donoho and Huo 2006) it is shown that by replacing the $L_0$-norm by the $L_1$-norm almost the same solution can be obtained as solving Eq. (5)

$$\hat{\boldsymbol{A}}_{\boldsymbol{1}} = \underset{\boldsymbol{A} \in \mathbb{R}^N}{\arg\min} \|\boldsymbol{A}\|_1 \qquad \text{subject to} \qquad \boldsymbol{y} = \boldsymbol{H} \cdot \boldsymbol{A} \tag{6}$$

The $L_1$-norm is the sum of all absolute values of the vector entries $A_j$

$$\|\boldsymbol{A}\|_1 = \sum_j |A_j| \tag{7}$$

Eq. (6) is now a convex optimization problem which can be solved by linear programming techniques. The reason why $L_1$-regularization also delivers sparse solutions, is illustrated in Fig. 1. It can be seen that $L_2$-regularization leads to a solution closest to the origin while $L_1$-regularization finds a solution on the coordinate axes, with just a few non zero elements.

## 3. Problem statement

In general, the dynamics of a nonlinear, time-varying structure can be described similar to Balageas *et al.* (2006) as

$$\begin{aligned} \boldsymbol{M}(\boldsymbol{\Theta}_k, \boldsymbol{x}_k, k)\ddot{\boldsymbol{x}}_k + g(\boldsymbol{\Theta}_k, \boldsymbol{x}_k, \dot{\boldsymbol{x}}_k, k) &= \boldsymbol{u}_k \\ \boldsymbol{\Theta}_{k+1} &= \boldsymbol{\Gamma}(\boldsymbol{\Theta}_k, \boldsymbol{x}_k, \dot{\boldsymbol{x}}_k, k) \\ \boldsymbol{y}_k &= \boldsymbol{h}^*(\boldsymbol{\Theta}_k, \boldsymbol{x}_k, \dot{\boldsymbol{x}}_k, k) \end{aligned} \tag{8}$$

The first line of Eq. (8) is the nonlinear equation of motion written for discrete time-steps $t_k = k\Delta t$, $k \in \mathbb{N}$. $M(\circ) \in \mathbb{R}^{m \times m}$ is the mass matrix and $g(\circ) \in \mathbb{R}^m$ the force vector of elastic and damping forces. These can depend on the nodal displacement $\boldsymbol{x} \in \mathbb{R}^m$, the nodal velocity $\dot{\boldsymbol{x}} \in \mathbb{R}^m$ and the time step $k$. The damage parameter $\boldsymbol{\Theta} \in \mathbb{R}^p$ describes the change of structural integrity (loss of stiffness, increase of damping, loss of mass, etc.) by location and damage extent. For structural health monitoring this is the parameter which needs to be reconstructed. Moreover, the damage parameter $\boldsymbol{\Theta}$ usually has also influence on the equation of motion. $\boldsymbol{u} \in \mathbb{R}^m$ is the vector of external loads acting on the structure. The number of degrees of freedom (DOF) is $m$. The nonlinear function $\boldsymbol{\Gamma} \in \mathbb{R}^p$ describes the evolution of the damage parameter in the second line of Eq. (8). Depending on the type of damage $\boldsymbol{\Gamma} \in \mathbb{R}^p$ can also a function of displacement and velocity. For example cracks grow faster if the vibration amplitude is large.

The third line of Eq. (8) is the measurement equation which links the model quantities (displacement, velocities and system parameters) with the output $\boldsymbol{y} \in \mathbb{R}^n$ of the measurement device by means of the function $\boldsymbol{h}^*(\circ) \in \mathbb{R}^n$. The number of measurements equals $n$.

If the structure can be assumed to be linear, the equation of motion becomes

$$\boldsymbol{M}(\boldsymbol{\Theta}_k)\ddot{\boldsymbol{x}}_k + \boldsymbol{C}(\boldsymbol{\Theta}_k)\dot{\boldsymbol{x}}_k + \boldsymbol{K}(\boldsymbol{\Theta}_k)\boldsymbol{x}_k = \boldsymbol{u}_k \tag{9}$$

Here, the structural mass $\boldsymbol{M}$, the structural stiffness $\boldsymbol{K}$ and the damping $\boldsymbol{C}$ still depend on the damage parameter $\boldsymbol{\Theta}$.

Mostly the evolution of the damage parameter $\boldsymbol{\Theta}$ and the structural dynamic vibrations occur on two different time scales. Compared to the structural vibrations, the evolution of damage is a rather slow process. Thus, the damage parameter $\boldsymbol{\Theta}$ seems to remain constant during a short time span of data acquisition (Balageas *et al*. 2006).

Now, a state space model can be defined, in which the unknown damage parameter vector is the state vector. The evolution of it is modeled by a Gaussian Markov process, also called random walk process (Ebrahimian *et al.* 2015)

$$\begin{aligned} \boldsymbol{\Theta}_{k+1} &= \boldsymbol{\Theta}_k + \boldsymbol{w}_k \\ \boldsymbol{y_k} &= \boldsymbol{h}\left(\boldsymbol{\Theta_k}, [\boldsymbol{U}]_k, \boldsymbol{x}_0, \dot{\boldsymbol{x}}_0, k\right) + \boldsymbol{v}_k, \end{aligned} \tag{10}$$

where $\boldsymbol{w}_k \in \mathbb{R}^p$ is zero-mean white process noise with covariance $\boldsymbol{Q}_k, \mathbf{w}_k \sim N(\mathbf{0}, \boldsymbol{Q}_k)$. Here, the measurement equation in the second line is defined slightly different as above. Unlike Eq. (8), the output measurement data are obtained depending on the initial nodal displacement and velocity $\boldsymbol{x}_0$ and $\dot{\boldsymbol{x}}_0$ and vector $[\boldsymbol{U}]_k = [\mathbf{u}_1, \ \mathbf{u}_2, \ \ldots \ , \mathbf{u}_k]^T$, which describes the external load input sequence from the first up to the current time step $k$. In this way, the (non-linear or linear) equation of motion can be implicitly included in the nonlinear measurement equation $\boldsymbol{h}(\circ) \in \mathbb{R}^n$. $\boldsymbol{v}_k \in \mathbb{R}^n$ represents the measurement noise with covariance $\boldsymbol{R}_k, \mathbf{v}_k \sim N(\mathbf{0}, \boldsymbol{R}_k)$. For reasons of clarity and without loss of generality in the remainder of this paper it is assumed that $\boldsymbol{x}_0 = \mathbf{0}$ and $\dot{\boldsymbol{x}}_0 = \mathbf{0}$.

## 4. Extended $L_1$-minimizing Kalman Filter

In the following, the new concept of $L_1$-minimizing sparse reconstruction is incorporated into an Extended Kalman Filter framework. Loffeld *et al.* (2016) were the first to propose an $L_1$-minimizing Kalman Filter approach for solving underdetermined sparse problems. Here, this idea is adopted to stabilize the Extended Kalman Filter parameter estimation process for a large damage parameter space $p$ and a low number of sensors $n$.

Structural damages due to e.g., cracks can often be interpreted as spatial singularities, as they lead to a stiffness reduction in a very local area of the system rather than a global stiffness reduction. Thus, it can be assumed that the unknown damage parameter vector $\boldsymbol{\Theta}$ is sparse. The sparsity will be considered as a constraint, which will be part of the state space model as an additional, nonlinear observation. It is promoted by the $L_1$-norm of the state vector

$$\hat{\boldsymbol{y}}_k = \gamma_k = \left\|\boldsymbol{\Theta_k}\right\|_1 = \sum_{j=1}^{p}\left|\Theta_{j,k}\right| \tag{11}$$

Starting from $\gamma_0 = \left\|\boldsymbol{\Theta}_0\right\|_1$ the fictive measurement $\gamma_k$ can now successively be decreased in each time step $k$ by a scaling factor $\alpha < 1$

$$\gamma_{k+1} = \alpha \left\|\boldsymbol{\Theta_k}\right\|_1 \tag{12}$$

The scalar Eq. (11) pushes down the $L_1$-norm of the state vector and thus leads to a sparse estimation of $\boldsymbol{\Theta}$. The now obtained augmented observation vector $\tilde{\boldsymbol{y}}_k$ reads as follows

$$\tilde{\boldsymbol{y}}_k = \begin{bmatrix} \boldsymbol{y}_k \\ \gamma_k \end{bmatrix} = \begin{bmatrix} \boldsymbol{h}\left(\boldsymbol{\Theta}_k, [\mathbf{U}]_k, k\right) \\ \left\|\boldsymbol{\Theta}_k\right\|_1 \end{bmatrix} + \begin{bmatrix} \boldsymbol{v}_k \\ \omega_k \end{bmatrix} \tag{13}$$

$\omega_k \in \mathbb{R}$ reflects the uncertainty of the additional $L_1$-minimizing observation equation.

For estimating the states of the now obtained nonlinear state space model an Extended Kalman Filter (EKF) is used. The EKF linearizes the nonlinear model in each time step around the *a posteriori* estimated state vector, using a first-order Taylor series approximation. After linearization the traditional prediction-correction algorithm of the Kalman Filter can be applied.

Starting from the initial conditions $\hat{\boldsymbol{\Theta}}_{0|0}$ and $\boldsymbol{P}_{0|0}$, a forecast of the state is made in the prediction step

$$\begin{aligned} \hat{\boldsymbol{\Theta}}_{k\,|\,k-1} &= \hat{\boldsymbol{\Theta}}_{k-1\,|\,k-1} \\ \boldsymbol{P}_{k\,|\,k-1} &= \boldsymbol{P}_{k-1\,|\,k-1} + \boldsymbol{Q}_k \end{aligned} \tag{14}$$

In the corrector step the current measurements $\boldsymbol{y}_k$ and the fictive measurements $\tilde{\boldsymbol{y}}_k$ are considered and compared with the prediction. The residual $\Delta\tilde{\boldsymbol{y}}_k$ is weighted by a Kalman matrix $\boldsymbol{K}_k$ and added to the prediction $\hat{\boldsymbol{\Theta}}_{k\,|\,k-1}$

$$\begin{aligned} \boldsymbol{y_k} &= \boldsymbol{h}\left(\hat{\boldsymbol{\Theta}}_{\boldsymbol{k|k-1}}, [\mathbf{U}]_k, k\right) \\ \boldsymbol{K_k} &= \boldsymbol{P}_{k|k-1}\boldsymbol{H}_k^T\left(\boldsymbol{H}_k\boldsymbol{P}_{k|k-1}\boldsymbol{H}_k^T + \tilde{\boldsymbol{R}}_k\right)^{-1} \\ \hat{\boldsymbol{\Theta}}_{k|k} &= \hat{\boldsymbol{\Theta}}_{k|k-1} + \boldsymbol{K}_k\,\Delta\tilde{\boldsymbol{y}}_k \\ \boldsymbol{P}_{k|k} &= \left(\mathbf{I} - \boldsymbol{K}_k\boldsymbol{H}_k\right)\boldsymbol{P}_{k|k-1} \end{aligned} \tag{15}$$

For the proposed damage parameter estimation strategy only the measurement equation is needs to be linearized

$$\boldsymbol{H}_k = \begin{bmatrix} \left.\dfrac{\partial \boldsymbol{h}\left(\boldsymbol{\Theta}_k, [\boldsymbol{U}]_k, k\right)}{\partial \boldsymbol{\Theta}}\right|_{\boldsymbol{\Theta}=\hat{\boldsymbol{\Theta}}_{k|k-1}} \\ \left.\dfrac{\partial\left\|\boldsymbol{\Theta}_k\right\|_1}{\partial \boldsymbol{\Theta}}\right|_{\boldsymbol{\Theta}=\hat{\boldsymbol{\Theta}}_{k|k-1}} \end{bmatrix} \tag{16}$$

---

**Input:** $[\mathbf{Y}]_k$, $[\mathbf{U}]_k$, $\hat{\boldsymbol{\Theta}}_0$, $\mathbf{P}_0$, $\mathbf{Q}$, $\tilde{\mathbf{R}}$, $\alpha$

$\hat{\boldsymbol{\Theta}}_{k-1} \leftarrow \hat{\boldsymbol{\Theta}}_0$

$\mathbf{P}_{k-1} \leftarrow \mathbf{P}_0$

**while** $k < k_{\max}$ **do**

  predictior step:

  $\hat{\boldsymbol{\Theta}}_k \leftarrow \hat{\boldsymbol{\Theta}}_{k-1}$

  $\mathbf{P}_k \leftarrow \mathbf{P}_{k-1}$

  corrector step:

  $\gamma_k \leftarrow \alpha \left\| \hat{\boldsymbol{\Theta}}_k \right\|_1$

  $[\hat{\mathbf{Y}}]_k^l \leftarrow \mathbf{h}^l\left(\hat{\boldsymbol{\Theta}}_k, [\mathbf{U}]_k, k, l\right)$

    *linearization:*

    $\mathbf{H}_k^1 \leftarrow \left.\frac{\partial \mathbf{h}^l(\boldsymbol{\Theta}_k, [\mathbf{U}]_k, k, l)}{\partial \boldsymbol{\Theta}}\right|_{\boldsymbol{\Theta}=\hat{\boldsymbol{\Theta}}_k}$

    $\mathbf{H}_k^2 \leftarrow \left[\mathrm{sign}(\hat{\Theta}_1), \mathrm{sign}(\hat{\Theta}_2), \cdots, \mathrm{sign}(\hat{\Theta}_p)\right]$

    $\mathbf{H}_k \leftarrow \left[(\mathbf{H}_k^1)^T, (\mathbf{H}_k^2)^T\right]^T$

    *residual:*

    $\Delta[\mathbf{Y}]_k^l \leftarrow [\mathbf{Y}]_k^l - [\hat{\mathbf{Y}}]_k^l$

    $\Delta\gamma_k \leftarrow \gamma_k - \|\hat{\boldsymbol{\Theta}}_k\|_1$

    $\Delta\tilde{\mathbf{y}}_k \leftarrow [(\Delta[\mathbf{Y}]_k^l)^T, \Delta\gamma_k]^T$

  $\mathbf{K}_k \leftarrow \mathbf{P}_k\mathbf{H}_k^T\left(\mathbf{H}_k\mathbf{P}_k\mathbf{H}_k^T +\right)^{-1} + \tilde{\mathbf{R}}$

  $\hat{\boldsymbol{\Theta}}_k \leftarrow \hat{\boldsymbol{\Theta}}_k + \mathbf{K}_k\Delta\tilde{\mathbf{y}}_k$

  $\mathbf{P}_k \leftarrow (\mathbf{I} - \mathbf{K}_k\mathbf{H}_k)\mathbf{P}_k$

  $k \leftarrow k + 1$

---

Fig. 2 Pseudo code of sparsity-constrained Extended Kalman Filter concept

The derivative of the measurement equation $\boldsymbol{h}(\circ)$ with respect to $\boldsymbol{\Theta}$ can be either approximated by the finite difference method or determined exactly by using the system-output sensitivity for linear structures. A detailed description of the output-sensitivity calculation can be found e.g., in (Fritzen *et al.* 1996) and is beyond the scope of this work. However, both methods require the structural model of the undamaged system and the input time history to linearize the measurement equation around the predicted state $\hat{\boldsymbol{\Theta}}_{k|k-1}$.

The Jacobian matrix of the $L_1$-minimizing constraint

$$\frac{\partial \|\boldsymbol{\Theta}\|_1}{\partial \boldsymbol{\Theta}} = \left[\frac{\partial \|\boldsymbol{\Theta}\|_1}{\partial \boldsymbol{\Theta}_1} \quad \frac{\partial \|\boldsymbol{\Theta}\|_1}{\partial \boldsymbol{\Theta}_2} \quad \cdots \quad \frac{\partial \|\boldsymbol{\Theta}\|_1}{\partial \boldsymbol{\Theta}_p}\right] \tag{17}$$

as second element of $\boldsymbol{H}_k$, can be obtained by

$$\frac{\partial \|\boldsymbol{\Theta}\|_1}{\partial \boldsymbol{\Theta}_\mathrm{j}} = \mathrm{sign}(\boldsymbol{\Theta}_\mathrm{j}) \tag{18}$$

The determination of the partial derivative in each time step $k$ is computationally very expensive. In order to save computing time, this can be performed just in every second or third step. This also helps to stabilize the filter process in the beginning.

As usual structural damage has no direct impact on the measurements at the same specific time step $k$, it is advisable to extend the physical measurement $\boldsymbol{y}_k$ and to process a bloc of $l$ physical measurements in each Kalman Filter step

$$[\mathbf{Y}]_k^l = \begin{bmatrix} \boldsymbol{y}_k \\ \boldsymbol{y}_{k+1} \\ \boldsymbol{y}_{k+2} \\ \vdots \\ \boldsymbol{y}_{k+l} \end{bmatrix} = \boldsymbol{h}^l(\boldsymbol{\Theta}_k, [\boldsymbol{U}]_k, k, l) + \boldsymbol{v}_k^l \tag{19}$$

By this *en bloc* processing, the filter is no longer operating in real time but with a time lag $t_l = l\Delta t$ in the past. *En bloc* processing also smoothes the predicted damage parameters. However, such an *en bloc* processing requires bigger measurement matrices, which leads to higher computational burden. The computational burden can limit the algorithm to offline monitoring. In the later simulation studies it has been shown that a moderate choice of $l$=50 is a good compromise between smoothing and computational burden.

Fig. 2 summarizes the implemented algorithm in pseudo code formulation.

## 5. Proof of concept

In order to demonstrate the functionality of the proposed damage identification strategy a proof of concept simulation study is performed. The observed mechanical structure is a simple square aluminum plate of 1 m × 1 m edge length and 2 mm thickness. It is clamped on all sides. The structural dynamics of the plate due to external forces are described by a finite element model. The plate is modeled by 121 quadratic shell elements and 144 nodes (each with 6 degrees of freedom), see Fig. 3.

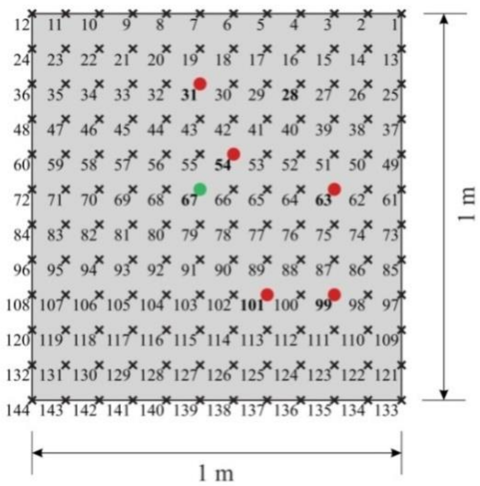


Fig. 3 Node numbering of the finite element plate model; node 31, 54, 63, 99 and 101 are acceleration measurement positions; node 67 is the excitation position

The employed structural responses are simulated acceleration measurements perpendicular to the plate plane. The obtained simulated measurement signals are low-pass filtered by a cut-off frequency of 200 Hz. Thus, for damage detection only the low frequency content of the time signals is employed. White Gaussian noise, with a standard deviation of three percent of the maximum measurement value, is added to the simulated outputs to imitate real acceleration measurement data. Throughout all investigations shown in this paper, only five accelerometers are used.

A widely used approach to introduce structural damage on a substructure or element level which represents the changes of the structural stiffness $\Delta\boldsymbol{K}$ compared to a reference model $\boldsymbol{K_0}$ is

$$\Delta\boldsymbol{K} = \sum_j \boldsymbol{K}_j \boldsymbol{\Theta}_j \tag{20}$$

where $\boldsymbol{K_j}$ is the $j$th substructure or element stiffness matrix, respectively. By determination of the unknown correction parameters $\boldsymbol{\Theta}=\left\lfloor \Theta_1 \quad \Theta_2 \quad \cdots \quad \Theta_p \right\rfloor$ the damage can be localized and quantified.

### 5.1 Single and multiple damage scenarios

In a first simulation study the stiffness of element no. 81 has been decreased by 20%. The plate structural vibration is excited by an impulse force load perpendicular to the plate surface at node no. 67 of known time history. Choosing the excitation node it is important that all modes of interest (here below 200 Hz) are excited. Beside this there are no other constrains concerning the number and placement of the active elements. The obtained simulated acceleration time data are now used for structural damage identification.

Fig. 4 shows the identification result, where the evolution of the damage parameter corresponding to element no. 81 is plotted overtime. It can be seen that starting from initial conditions (all damage parameters zero) the parameter of the damage element tends to the true value of stiffness reduction. Fig. 5 shows that for all the other elements the corresponding damage parameters are close to zero. Thus, the damage is localized and quantified.

Figs. 6 and 7 compare the damage parameter estimation results for the proposed Extended Kalman Filter method with and without additional $L_1$-minimizing observation. It is obvious that no clear damage estimation result can be achieved without $L_1$-minimizing observation. Even though the reconstructed damage parameter error for the damage element no. 81 is not too big, many more element stiffness changes (reduction and increase) are identified. On the other hand, it can be clearly distinguished between damaged and undamaged elements if the additional observation is used, as $L_1$-minimization promotes this sparse solution. In a next step a multiple damage scenario is investigated. Here the plate structural damage is modeled by a stiffness reduction of various elements with different amount. Which means the damage parameter vector needs to be slightly dense than in the case of a single element stiffness change.

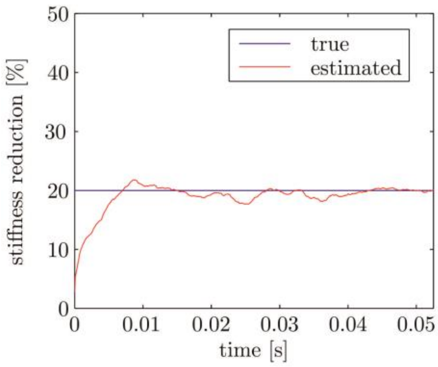


Fig. 4 Damage identification result; evolution of damage parameter no. 81

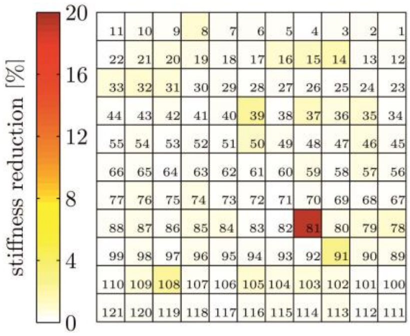


Fig. 5 Estimated stiffness reduction pattern at the end of simulation time

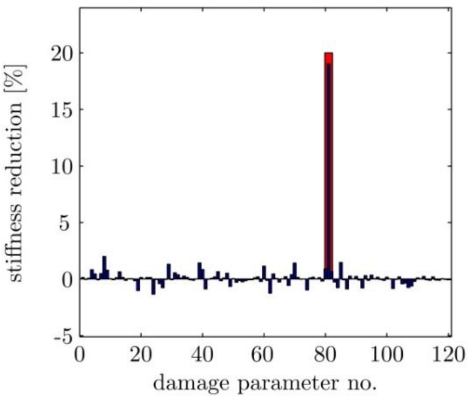


Fig. 6 Kalman Filter estimation without additional $L_1$-observation

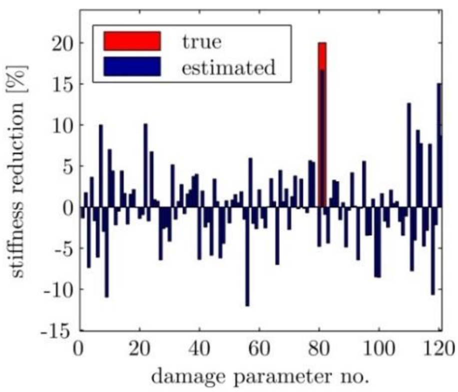


Fig. 7 Estimation result with $L_1$ -minimizing observation

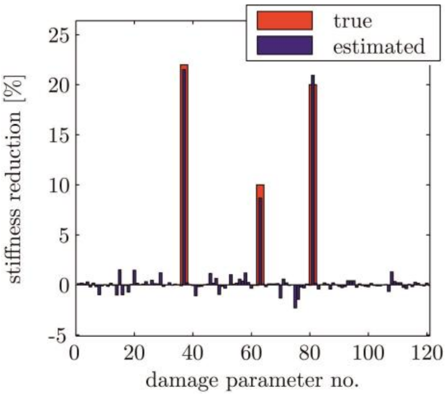


Fig. 8 Multiple damage scenarios: three damaged elements

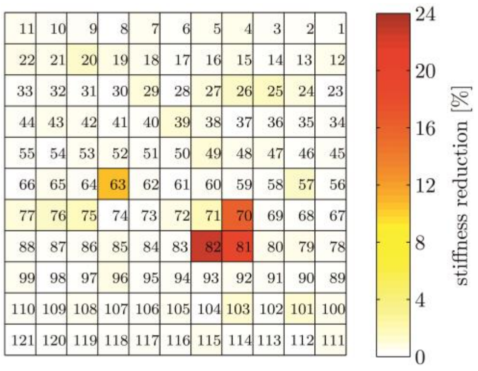


Fig. 9 Damage identification result for larger damaged areas

Fig. 8 shows the damage identification results at the end of simulation time for three damaged elements. In this case a clear damage identification, similar as before is obtained.

In Fig. 9 a damage scenario is simulated and reconstructed in which a larger area is damaged by means of an element stiffness reduction. The element stiffness of element no. 63, 70, 81 and 82 is reduced. The identified damage pattern shown in Fig. 7 agrees with the true one. Beside the actual damage elements, only a few other elements show a negligible stiffness change.

### *5.2 Monte Carlo simulation*

In section 5.1 some selected damage identification results have been shown. However, for a statistical validation a Monte Carlo simulation is performed. 5000 trials with different damage scenarios are carried out. In each of the 5000 trials a single damage is introduced in the structure by reducing the stiffness of one element. The damage location is chosen randomly with uniform distribution over all elements. The damage extent is also a random parameter with Gaussian distribution (mean value: 25% stiffness reduction; standard deviation: 5%). As before, white Gaussian noise, with a standard deviation of three percent of the maximum measurement value is added to the simulated outputs.

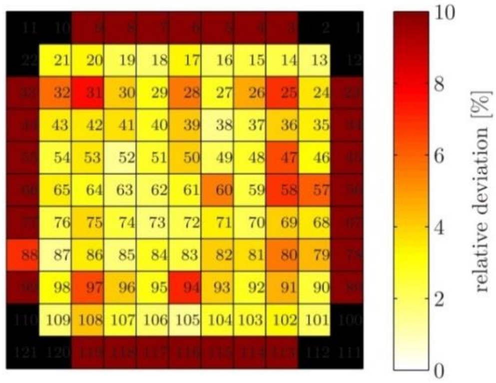


Fig. 10 Results of Monte Carlo simulation

The obtained results by using the proposed algorithm are displayed in Fig. 10. For each element, Fig. 10 shows the mean value of the relative deviation for damage extent estimation. The results indicate clearly a bad performance of estimation a damage, which is introduced in a boundary element. As the plate is clamped on all sides, vibration-based damage detection is very difficult for such elements placed at the clamped edges. Nevertheless, the damage extends estimation for the inner plate elements are very reliable. The mean estimation error is distinctly under 10%. Moreover, the damage location for an inner plate element stiffness reduction is always detected correctly.

### *5.3 Model error compensation*

As the proposed damage identification strategy is a model-based approach, modeling errors will have an impact on the reconstruction results. For most practical applications there are some modeling parameters which are subject to uncertainties, e.g., the global modulus of elasticity, the mass density or the correct definition of the boundary conditions.

In order to compensate possible modeling errors, such model parameters can also be integrated in the estimation process. This requires the explicit knowledge of model parameters, which are subject to deviations. Thus, the parameter vector $\boldsymbol{\Theta}$ needs to be extended by these model parameters

$$\boldsymbol{\Theta} = \left[\Theta_1, \Theta_2, \cdots, \Theta_p, \Theta_1^m, \cdots, \Theta_n^m\right] \tag{21}$$

The algorithm will fit the unknown model parameters to the measurement output data. Here the first $p$ values are the damage parameters as previously defined. The last $n$ parameters describe now the global model parameters.

In the following simulation study the filter model used for the reconstruction process varies from the one, which is employed to create the measurement data, not only in terms of the structural damage but also in terms of a modulus of elasticity and mass density. Therefore, two additional parameters $\boldsymbol{\Theta}_n^m$ ($n$=2) needs to be estimate

$$\Delta \boldsymbol{K} = \Theta_1^m \boldsymbol{K} \quad \text{and} \quad \Delta \boldsymbol{M} = \Theta_2^m \boldsymbol{M} \tag{22}$$

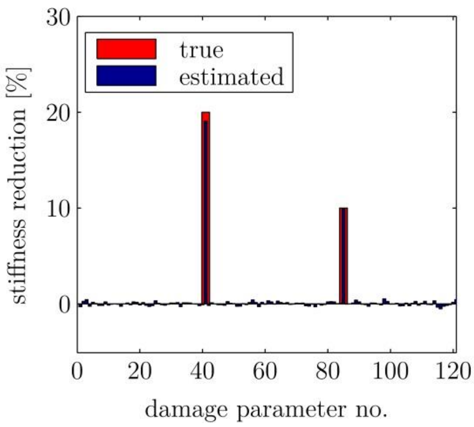


Fig. 11 Damage identification by using an incorrect structural model

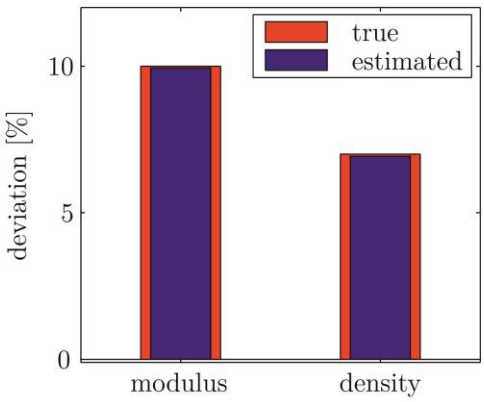


Fig. 12 Estimation of initially wrong model parameters (Young's modulus and mass density)

Fig. 11 shows a damage reconstruction result by using an incorrect structural model. The deviation is 7% in mass density and 10% in modulus. However, a very clear estimation of the damage pattern can be obtained. The damage elements no. 41 and 85 are identified correctly and also the damage extend is reconstructed properly. Additionally, the model parameter mass density and modulus of elasticity have been identified, as shown in Fig. 12.

## 6. Conclusions

In this contribution a new time domain method for damage detection has been proposed. The local character of damage justifies the use of sparse reconstruction strategies for the ill-posed inverse problem. Sparsity of the estimated state vector of damage parameters is ensured within the Extended Kalman Filter by adding a fictive non-linear $L_1$-minimizing observation.

The structural model description presented in section 3 allows to analyze various types of structures. Therefore, the proposed approach is not limited to aluminum structures, as shown in section 5. Due to the required linearization process it is even possible to monitor structures with nonlinear behavior. Moreover, the approach can be extended to detected different types of damages (e.g., breathing cracks), if a corresponding damage model is integrated in the system description.

It has been shown in this paper that the proposed reconstruction method is able to determine the damage due to local stiffness reductions by position and extent simultaneously. In contrast to the Extended Kalman Filter process without additional $L_1$-observation a clear damage pattern is obtained. This was shown for single damage scenarios as well as for multiple damage events. A statistical validation has been performed by means of a Monte Carlo simulation. Considering the damage parameter space of size 121 in the demonstrated study, the number of sensors using only five accelerometers is significantly lower than the parameter space. Moreover, modeling error can be compensated by including the model parameters, which are subject to uncertainties. Besides the unknown model parameter, this approach can also be used to reconstruct damage under changing environmental and operational conditions (EOC), if the EOC sensitive parameters are also included in the parameter vector.

The sparsity-constrained Extended Kalman Filter concept is a promising approach for time domain structural damage identification as the required measurement information can be significantly reduced. However, to operate this methodology on a real structure several additional investigations needs to be carried out under real environmental conditions. Amongst other things the influence of environmental perturbations and unrecognized model errors must be analyzed in a long term study.

A drawback of this method is clearly the fact, that the excitation signal time history needs to be known. Large additional excitations (e.g., environmental perturbations) may lead to deviations of the reconstruction results.

## References

Balageas, D., Fritzen, C.P. and Güemes, A. (2006), *Structural Health Monitoring*, Hermes Science Publishing

Candés, E.J. and Wakin, E.J. (2008), "An introduction to compressive sampling", *IEEE Signal Proc. Mag.*, **25**(2), 21-30.

Ching, J., Beck, J.L. and Porter, K.A. (2006), "Bayesian state and parameter estimation of uncertain dynamical systems", *Probab. Eng. Mech.*, **21**(1), 81-96.

Corigliano, A. and Mariani, S. (2004), "Parameter identification in explicit structural dynamics: performance of the extended Kalman filter", *Comput. Method. Appl. M.*, **193**(36-38), 3807-3835.

Ding, Y. and Gua, L. (2016), "Structural identification based on incomplete measurements with iterative Kalman filter", *Struct. Eng. Mech.*, **59**(6), 1037-1054.

Donoho, D.L. and Huo, X. (2006), "Uncertainty principles and ideal atomic decomposition", *IEEE T. Inform. Theory*, **47**(7), 2845-2862.

Ebrahimian, H., Astroza, R. and Conte, J.P. (2015), "Extended Kalman filter for material parameter estimation in nonlinear structural finite element models using direct differentiation method", *Earthq. Eng. Struct. D.*, **44**(10), 1495-1522.

Fritzen, C.P. and Ginsberg, D. (2017), "Sparse solution techniques in load and damage monitoring systems", *Advances in Science*

*and Technology, 7th Forum on New Materials – Part E.*, **101**, 35-44.
Fritzen, C.P., Jennewein, D. and Buchen, D. (1996), "Model Based Damage Detection From Vibration Data", *Proc. ISMA21: Noise and Vibration Engineering*, 1017-1032.
Lei, Y., Liu, C., Jiang Y.Q. and Mao, Y.K. (2013), "A two-stage and two-step algorithm for the identification of structural damage and unknown excitations: numerical and experimental studies", *Smart Struct. Syst.*, **15**(1), 57-80.
Lei, Y., Chen, F. and Zhou, H. (2015), "Substructure based structural damage detection with limited input and output measurements", *Smart Struct. Syst.*, **12**(6), 619-640.
Liu, X., Escamilla-Ambrosio, P.J. and Lieven, N.A.J (2009), "Extended Kalman filtering for the detection of damage in linear mechanical structures", *J. Sound Vib.*, **325**(4-5), 1023-1046.
Loffeld, O., Seel, A., Conde, M.H. and Wang, L.A. (2016), "Nullspace based L1 minimizing Kalman Filter approach to sparse CS Reconstruction", *Advances in Sience and Technology, 11th European Conference on Synthetic Aperture Radar (EUSAR 2016)*
Sato, T. and Qi, K. (1998), "Adaptive H∞ filter: its application to structural identification", *J. Eng. Mech. - ASCE*, **141**(11), 1233-1240.
Smyth, A.W., Masri, S.F., Chassiakos A.G. and Caughey, T.K. (1999), "On-line parametric identification of MDOF nonlinear hysteretic systems", *J. Eng. Mech. - ASCE*, **125**(2), 133-142.
Sohn, H., Farrar, C.R., Hemez, F.M., Shunk, D.D., Stinemates, D.W., Nadler, B.R. and Czarnecki, J.J. (2003), A Review Of Structural Health Monitoring Literature: 1996-2001, *Los Alamos National Laboratory*
Tikhonov, A.N. and Arsenin, V.I.A. (1977), "Solutions of ill-posed problems", *Scripta series in mathematics*.
Wan, C., Sato, T., Wu, Z. and Zhang, J. (2013), "Damage identification using chaotic excitation", *Smart Struct. Syst.*, **11**(1), 87-102.
Wu, B. and Wang, T. (2014), "Model updating with constrained unscented Kalman filter for hybrid testing", *Smart Struct. Syst.*, **14**(6), 1105-1129.
Yang, J.N. and Lin, S. (2005), "Identification of parametric variations of structures based on least squares estimation and adaptive tracking technique", *J. Eng. Mech. - ASCE*, **131**(3), 290-298.
Zhang, C., Huang, J.Z., Song, G.Q., Dai, L. and Li, H.K. (2016), "Detection of structural damage via free vibration responses by extended Kalman filter with Tikhonov regularization scheme", *Struct. Monit. Maint.*, **3**(2), 115-127.

*FC*